

## Structural Origins of Magnetic Anisotropy in Sputtered Amorphous Tb-Fe Films

V. G. Harris, K. D. Aylesworth, B. N. Das, W. T. Elam, and N. C. Koon

*Naval Research Laboratory, Washington, D.C. 20375-5000*

(Received 11 May 1992)

Using x-ray-absorption fine-structure measurements we have obtained clear evidence for structural anisotropy in amorphous sputter-deposited TbFe films exhibiting perpendicular magnetic anisotropy. Modeling of the data shows that perpendicular anisotropy in these films is associated with Fe-Fe and Tb-Tb pair correlations which are greater in plane and Tb-Fe correlations which are greater perpendicular to the film plane. Upon annealing at 300°C the measured structural anisotropy disappears and the magnetic anisotropy decreases to a level consistent with magnetoelastic interactions between the film and substrate.

PACS numbers: 61.10.Lx, 75.30.Gw, 75.50.Kj, 75.70.-i

Perpendicular magnetic anisotropy in amorphous rare-earth-transition-metal (RE-TM) films was first observed in sputtered Gd-Co by Chaudhari, Cuomo, and Gambino of IBM in 1973 [1]. Since that time amorphous TbGdFeCo alloy films have become key materials for use in the latest generation of high capacity magneto-optic memory storage devices, with one of the most important features being sufficient perpendicular magnetic anisotropy to maintain the magnetization direction perpendicular to the plane of the film. Although extensive experimental studies have defined the empirical relationships between film composition, preparation conditions, and the observed properties such as magnetization, anisotropy, coercivity, and Curie temperature, the underlying mechanisms responsible for the observed characteristics have not yet been unambiguously established. There have been many discussions as to the possible mechanisms which contribute to magnetic anisotropy, i.e., magnetostriction [2], bond-orientational anisotropy [3], anisotropic pair correlations [4], dipolar effects [5,6], and growth induced structural anisotropy [7], although choosing between the various ideas has been made difficult by the lack of adequate structural information.

In the present work we have used conversion-electron extended x-ray-absorption fine structure (EXAFS) to study the short-range structure of several  $Tb_xFe_{1-x}$  films prepared by conventional ion beam sputtering. To obtain anisotropic structural information we made use of the fact that the photoelectrons have a distribution weighted according to  $\cos^2\alpha$ , where  $\alpha$  is the angle between the electric field vector of the incident radiation and the direction of the ejected photoelectron. We observe a well-defined anisotropic fine structure above both the Fe and Tb absorption edges. By standard EXAFS modeling techniques we have been able to estimate independently for each specie of atom the coordination and radial distance of the near-neighbor atomic shells as a function of film composition, annealing temperature, and direction relative to the film plane, thus obtaining a very detailed picture of the short-range structural anisotropy. One of the central results is that perpendicular anisotropy in these

films is associated with Fe-Fe and Tb-Tb near-neighbor correlations which are greater in-plane and Tb-Fe near-neighbor correlations which are greater perpendicular to the film plane.

Three  $Tb_xFe_{1-x}$  ( $x=0.18, 0.23, 0.26$ ) alloy films were sputtered at room temperature onto glass substrates using a Kaufman-type ion source. Films were deposited at rates of 2–2.5 Å/sec to a thickness of 2800 Å with a protective overcoat of 180 Å Ge. Magnetic measurements were performed using a vibrating sample magnetometer. All three films were found to have strong perpendicular magnetic anisotropy. Their room-temperature anisotropy energies ranged from  $(0.8 \text{ to } 1.6) \times 10^6 \text{ erg/cm}^3$ , which is consistent with previous results on similar films [2].

X-ray absorption spectra encompassing both the Fe K and the Tb  $L_{III}$  absorption edges were collected on the Naval Research Laboratory's materials analysis beamline, X23B, at the National Synchrotron Light Source (NSLS). Data were collected at room temperature using an electron-detection technique [8] with the incident synchrotron radiation aligned at a 90° and an 8°–10° glancing angle relative to the sample plane. Because of the  $\cos^2\alpha$  weighting of the EXAFS signal the normal-incidence data primarily reflect atomic structure in the film plane, while the glancing angle data reflect structure in the perpendicular direction. Because the limiting factor in the data was signal to noise in the Tb EXAFS, most of the results quoted in this paper are for the 26% Tb film.

Following established EXAFS analysis procedures [9] the fine structure was normalized to the edge step height and a cubic spline fit was used to remove the nonoscillatory background. The data were then converted to photoelectron wave-vector space. Figure 1 presents a comparison of Fe EXAFS data for the  $Tb_{0.26}Fe_{0.74}$  alloy film collected with normal and glancing incidence radiation. The existence of structural anisotropy in the data is clearly seen above the noise level as a difference in peak-to-peak amplitude of the first two periods of EXAFS oscillations. Figures 2(a) and 2(b) present Fourier-transformed data (uncorrected for electronic phase shifts) for the Fe EX-

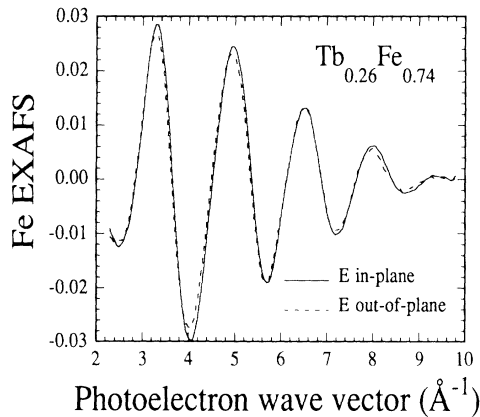


FIG. 1. Fe EXAFS data after background removal and conversion to photoelectron wave-vector space for the electric field vector ( $\mathbf{E}$ ) aligned parallel and perpendicular to the film plane.

AFS data presented in Fig. 1 and similar Tb EXAFS data acquired from the same sample. Because we were primarily concerned with the differences between the structure along the directions parallel and perpendicular to the film plane, the normal and glancing incidence data were transformed with an identical  $k$ -space range and transform parameters. Error bars on inset data represent both statistical and parameter analysis.

The large peaks near 2 Å for the Fe data and 2.4 Å for the Tb data in Figs. 2(a) and 2(b) contain information on the number of near-neighbor atoms, their radial distance, and static and dynamic disorder of their atomic shells. The lack of structure above the noise level at radial distances beyond the near-neighbor peak is indicative of the lack of sharply defined interatomic distances beyond the nearest neighbors. The differences between data sets for normal and glancing incidence are quite evident in both the Fe and Tb transforms as changes in amplitude and shape of the near-neighbor Fourier peak. This clearly implies that the short-range structure around both Fe and Tb is anisotropic relative to the film plane. In order to determine the nature of this anisotropy, however, it is necessary to quantitatively model the data.

The data were compared with theoretical EXAFS

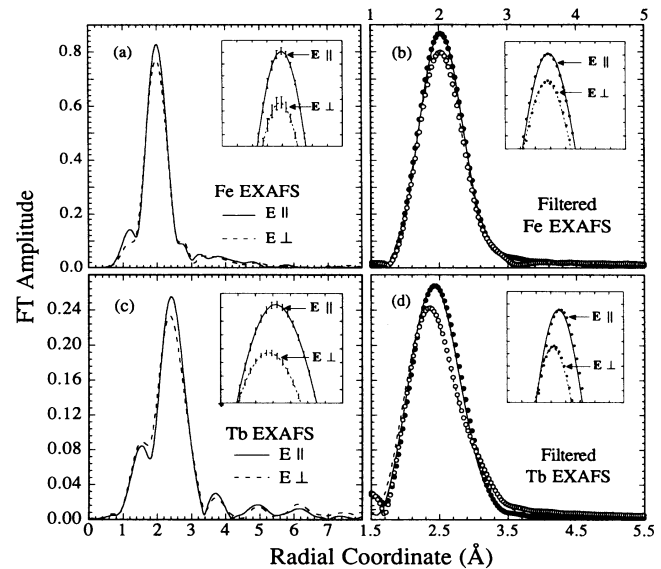


FIG. 2. Fourier-transformed EXAFS data for Fe (a) and Tb (c). Error bars in the magnified inset data are from a statistical and parameter variation analysis. (b) and (d) represent filtered EXAFS data compared to theoretically calculated fits ( $\bullet$ ,  $\mathbf{E} \parallel$ ;  $\circ$ ,  $\mathbf{E} \perp$ ).

curves calculated using FEFF codes (version 3) [10]. The fitting process was carried out in wave-vector space using data back transformed from a window in the  $r$ -space plot which included the near-neighbor Fourier peak. This procedure is effective in isolating those data which contribute to the near-neighbor environment of the absorbing atom. The amplitude reduction factor ( $S_0^2$ ) used in the calculations were obtained by fitting experimental EXAFS data collected from a  $\text{TbFe}_2$  powder standard. The amorphous film data were fit by adjusting the coordination number, radial distance, and Debye-Waller coefficient of atomic shells surrounding the absorbing atom. After extensive modeling trials we found that a multiple shell environment of two Fe shells and a single Tb shell around each atom fits the data quite well, as illustrated in Figs. 2(c) and 2(d). The parameters used to obtain the calculated data for  $\text{Tb}_{0.26}\text{Fe}_{0.74}$  are listed in Table I. For those parameters which are coupled, the error estimates correspond to the ranges of parameters which keep the  $\chi^2$

TABLE I. Calculated coordination numbers (CNs) deduced from modeling of Fe and Tb EXAFS data for  $\text{Tb}_{0.26}\text{Fe}_{0.74}$  sample. Quoted error limits maintain  $\chi^2$  within 10% of the best-fit value.  $\parallel$ : electric field vector oriented in the plane of the sample;  $\perp$ : electric field vector oriented near perpendicular to the plane of the sample.

	$r$ (Å)	$\Delta\sigma_{300\text{K}}^2$	CN $^{\parallel}$	CN $^{\perp}$	CN $^{\parallel}$ -CN $^{\perp}$	CN $^{\parallel-\perp}$
Fe-Fe	$2.46 \pm 0.005$	$0.006 \pm 0.0004$	$4.94 \pm 0.09$	$4.4 \pm 0.15$	0.54	1.44
Fe-Fe	$2.64 \pm 0.01$	$0.001 \pm 0.0004$	$1.5 \pm 0.16$	$1.57 \pm 0.15$	-0.07	-0.54
Fe-Tb	$3.00 \pm 0.02$	$0.013 \pm 0.002$	$1.35 \pm 0.25$	$1.85 \pm 0.25$	-0.55	-1.06
Tb-Fe	$2.84 \pm 0.005$	$0.012 \pm 0.0007$	$4.46 \pm 0.18$	$4.27 \pm 0.15$	0.19	1.06
Tb-Fe	$3.04 \pm 0.01$	$0.010 \pm 0.001$	$2.60 \pm 0.16$	$3.4 \pm 0.18$	-0.80	-2.3
Tb-Tb	$3.5 \pm 0.06$	$0.03 \pm 0.015$	$3.5 \pm 1$	$2.5 \pm 1$	1	1.6

parameter to within 10% of the best-fit value. The differences between fits for directions parallel and perpendicular to the plane were reflected almost entirely by changes in the occupation numbers—the radial distances and Debye-Waller factors were essentially unchanged. It is interesting to note that two shells of Fe close together provide a much better fit to the data than a single broader shell. We speculate that this is because the pair-correlation functions peak sharply with radial distance at approximately the sum of the Goldschmidt radii and then decrease more slowly with distance due to trapped volume effects.

Two different methods of analysis were used to estimate the anisotropy between the in-plane and out-of-plane atomic structure. First was independent modeling of the data collected at the two sample orientations as just described. As a consistency check the incident and glancing angle data sets were subtracted after the analysis had been carried through to the back-Fourier-transformed stage. This difference spectrum was then modeled as described in the previous paragraph, yielding directly the differences between coordination numbers in the parallel and perpendicular directions (last column of Table I). This fit of the difference data shows the same qualitative structural anisotropy as the differences between the fits of separate data sets, although with somewhat larger numerical changes. In both cases the changes with orientation are well outside the statistical and fitting uncertainties.

An important test of the results presented here is to determine what happens to the structural anisotropy when the samples are annealed at temperatures in the range of 200–300°C, which is known to substantially reduce the perpendicular magnetic anisotropy energy [11]. Annealing the  $\text{Tb}_{0.26}\text{Fe}_{0.74}$  film at a temperature of 300°C for a period of 1 h resulted in reduction of the magnetic anisotropy energy of over 80% from  $1.6 \times 10^6$  erg/cm<sup>3</sup> to  $0.3 \times 10^6$  erg/cm<sup>3</sup>, which is comparable to the value expected from magnetoelastic interactions between the film and substrate [2]. Figure 3 shows the Fourier transforms of the Fe EXAFS data for this sample after the 300°C heat treatment. The anisotropy seen in Fig. 2(a) for the as-deposited sample has been completely eliminated by the 300°C anneal. Similar behavior was observed in the Tb EXAFS data. This suggests that essentially all of the structural anisotropy has been removed by annealing and the residual anisotropy is most likely due solely to magnetoelastic effects.

The results presented in Table I provide a very detailed picture of the structural anisotropy which exists in an amorphous  $\text{Tb}_{0.26}\text{Fe}_{0.74}$  film with perpendicular magnetic anisotropy. If we adopt the view that the two near-neighbor iron shells are really a way of representing a single broadened asymmetric shell, then we conclude that both the Tb-Tb and Fe-Fe near-neighbor correlations are greater in the film plane, while the Tb-Fe correlations are

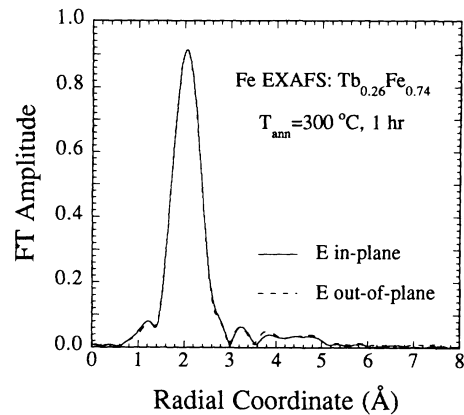


FIG. 3. Fourier-transformed Fe EXAFS data for a  $\text{Tb}_{0.26}\text{Fe}_{0.74}$  alloy film heat treated at 300°C for 1 h. The structural anisotropy seen in Fig. 2(a) has been eliminated by the annealing.

greater in the perpendicular direction. From the population shifts between the near-neighbor iron shells we can also infer that the average near-neighbor Fe-Fe and Fe-Tb distances are very slightly less in-plane than out-of-plane, although the shifts are comparable to the uncertainties in the fits. The shifts in the occupation numbers of the various shells, however, are greater than the statistical uncertainties inherent in the data reduction and fitting process and the Fe and Tb results taken separately give consistent results. Supporting information for the reliability of the occupation numbers comes from the observation that they behave properly with composition for the three films analyzed and from the fact that two very different methods of analysis yield similar results. Furthermore EXAFS data on annealed films expected to be structurally isotropic yield identical spectra and thus identical occupation numbers for the normal and glancing incidence directions.

These results represent the most detailed anisotropic structural information yet obtained for amorphous rare-earth-transition-metal alloy films with perpendicular magnetic anisotropy, and the annealing experiment clearly demonstrates that the measured structural and magnetic anisotropy are strongly correlated.

We are thankful to Professor J. J. Rehr and associates (University of Washington) for providing us with the FEFF codes used here in modeling of the EXAFS data. This research was carried out, in part, at the National Synchrotron Light Source (Brookhaven National Laboratories, Upton, NY), which is sponsored by the U.S. Department of Energy (Division of Material Science and Division of Chemical Sciences of the Office of Basic Energy Sciences). V.G.H. and K.D.A. acknowledge support from the National Research Council-Naval Research Laboratory research associate program.

[1] P. Chaudhari, J. J. Cuomo, and R. J. Gambino, IBM J.

- Res. Dev. **17**, 66 (1973); Appl. Phys. Lett. **22**, 337 (1973).
- [2] S.-C. N. Cheng, M. H. Kryder, and M. C. A. Mathur, IEEE Trans. Magn. **25**, 4018 (1989).
- [3] X. Yan, M. Hirscher, T. Egami, and E. E. Marinero, Phys. Rev. B **43**, 9300 (1991).
- [4] R. J. Gambino and J. J. Cuomo, J. Vac. Sci. Technol. **15**, 296 (1978).
- [5] T. Mizoguchi and G. S. Cargill, III, J. Appl. Phys. **50**, 3570 (1979).
- [6] H. Fu, M. Mansuripur, and P. Meystre, Phys. Rev. Lett. **66**, 1086 (1991).
- [7] F. Hellman and E. M. Gyorgy, Phys. Rev. Lett. **68**, 1391 (1992).
- [8] W. T. Elam, J. P. Kirkland, R. A. Neiser, and P. D. Wolf, Phys. Rev. B **38**, 26 (1988).
- [9] See, for example, D. E. Sayers and B. A. Bunker, in *X-Ray Absorption: Basic Principles of EXAFS, SEXAFS, and XANES*, edited by D. C. Koningsberger and R. Prins (Wiley, New York, 1988).
- [10] J. J. Rehr, J. Mustre de Leon, S. I. Zabinsky, and R. C. Albers, J. Am. Chem. Soc. **113**, 5135 (1991).
- [11] P. Hansen, G. Clausen, G. Much, M. Rosenfranz, and K. Witter, J. Appl. Phys. **66**, 756 (1989).